Print ISSN: 0375-9237
Online ISSN: 2357-0350

EGYPTIAN JOURNAL OF BOTANY (EJBO)

Impact of Metallo-antifungals on growth and virulence genes across *Candida* species

Rania K. Mohammed, Mohammed E. Dawoud, Tharwat E. Radwan, Dina M. Bassiouny, Hoda M. Shehata, Rehab M. Hafez

PUBLISHED BY
THE EGYPTIAN
BOTANICAL SOCIETY

Impact of Metallo-antifungals on growth and virulence genes across *Candida* species

Rania K. Mohammed[1], Mohammed E. Dawoud[1], Tharwat E. Radwan[2], Dina M. Bassiouny[3], Hoda M. Shehata[1], Rehab M. Hafez[1]

[1]*Botany and Microbiology Department, Faculty of Science, Cairo University, Giza, Egypt*
[2]*Botany and Microbiology Department, Faculty of Science, Fayoum University, Fayoum, Egypt*
[3]*Clinical Pathology Department, Faculty of Medicine, Cairo University, Giza, Egypt*

Candida species, particularly *Candida albicans* and *Candida tropicalis*, are virulent and frequent, leading to severe systemic and superficial infections, particularly in those with weakened immune systems. This study investigated the antifungal impact of both single and combined metal ions and how they affect the expression of virulence genes. PCR-based identification confirmed the presence of *C. albicans* (109 bp) and *C. tropicalis* (110 bp). Different species of *Candida* (*C. albicans* and *C. tropicalis*) were treated with serial dilutions of 0.1 M of various metal ions (B^{+}, Fe^{2+}, or Fe^{3+}, Co^{2+}, Ni^{2+}, Cu^{+}, or Cu^{2+}, Zn^{2+}, Mo^{6+}, and Cr^{6+}) singly and their antifungal activities were estimated through inhibition zone diameters (IzD). According to single metal treatments, chromium had the highest inhibition zone (IzD = 19 mm) against both *Candida* spp. followed by molybdenum and then cobalt. Also, the Co/Mo combination (IzD = 24 mm) revealed the highest inhibitory effect. The Co/Mo mixture showed potent antifungal properties at 58.93 µg/mL and 95.95 µg/mL, with no fungicidal effect below 0.1 M, as confirmed by disc diffusion and microdilution assays. PCR analysis of virulence genes revealed the presence of *HWP1*, *SAP4*, and *HYR1* genes. The Co/Mo1 combination effectively inhibits *Candida* growth by downregulating *HWP1*, *HYR1*, and *SAP4* genes in *C. albicans* and suppressing *ALS1* and *PLB1* genes in *C. tropicalis*. These results demonstrate that the Co/Mo1 treatment is a promising antifungal agent that efficiently inhibits the growth of both *Candida* spp. and suppresses their essential virulence genes.

Keywords: *Candida albicans*, *Candida tropicalis*, metals, virulence genes, pathogenicity, gene expression

ARTICLE HISTORY
Submitted: March 12, 2025
Accepted: May 24, 2025

CORRESPONDENCE TO
Rania K. Mohammed,
Botany and Microbiology Department,
Faculty of Science, Cairo University,
Giza, Egypt
Email: khodierrania@gmail.com
DOI: 10.21608/ejbo.2025.360160.3223

EDITED BY: N. Khalil

INTRODUCTION

Over the past decades, infections caused by *Candida* species have significantly increased due to factors like the AIDS epidemic, aging populations, and the rise in the number of immunocompromised patients. Although non-*C. albicans Candida* (NCAC) species such as *C. glabrata*, *C. tropicalis*, and *C. parapsilosis* are now recognized as pathogens, *C. albicans* remain the primary cause of candidosis. The pathogenicity of *Candida* species is linked to virulence factors such as adhesion to host surfaces, biofilm formation, and secretion of hydrolytic enzymes. Advanced identification techniques have also contributed to the rising recognition of these species as pathogens (Silva *et al.,* 2012).

C. albicans is commonly isolated from both healthy and diseased individuals. Its polymorphic nature, indicated by being "germ tube positive," is a diagnostic marker (Klesiewicz *et al.,* 2023). Improved molecular techniques have led to the discovery of new species and increased understanding of their role in human infections (Gácser *et al.,* 2007a, b). Epidemiological studies indicate *C. tropicalis* as the second most recovered species in candidemia cases, especially in intensive care units and in patients with malignancy or prolonged catheter use (Colombo *et al.,* 2007). It is frequently isolated in neutropenic patients and has the highest genetic similarity to *C. albicans* (Butler *et al.,* 2009).

Candidosis, candiduria, and candidemia represent infections by *Candida* species affecting different body areas with varied severity. Candidosis includes infections like oral thrush and vaginal candidiasis, generally localized but potentially spreading if untreated. Candiduria indicates *Candida* presence in urine, often asymptomatic but requiring treatment in high-risk patients. Candidemia is a severe systemic infection with symptoms like fever and chills, which can lead to sepsis and organ dysfunction if untreated, demanding urgent antifungal therapy (Pappas *et al.,* 2016).

Metallo-antifungals, containing metal ions or complexes, offer a promising alternative to conventional antifungal therapies due to rising antifungal resistance. These metal ions (CrO_4^{2-}, Co^{2+}, Cu^{2+}, Ag^{+}, Zn^{2+}, Cd^{2+}, Hg^{2+}, Pb^{2+}, AsO^{2-}, and SeO_3^{2-}) influence biofilm structure and morphogenesis in *Candida* species, preventing yeast-to-hyphal transitions and influencing virulence and resistance (Chandra *et al.*, 2001). How *C. albicans* and *C. tropicalis* interact with metal ions may represent an essential biotic-abiotic interaction. Metal ions can alter biofilm sensitivity to antifungal treatments, potentially suppressing disease progression and shifting the *Candida* community from commensalism to pathogenicity, highlighting their potential as therapeutic agents and environmental stress markers (Černáková and Rodrigues, 2020).

Candida species have key virulence factors, including adhesion molecules, hydrolytic enzymes, and signaling pathways. The *ALS* gene family is associated with pathogenic mechanisms in *C. albicans*, with strain and allele level variability. *ALS1* and *ALS3*, proteins involved in adhesion, are essential in biofilm formation, regulated by *Bcr1*. Also, *HWP1*, encoding cell wall protein, is crucial for hyphal development and adhesion to host cells (Orsi *et al.*, 2014).

In addition, the *RAS1* protein, through guanine triphosphate binding and lipid modifications, regulates processes like biofilm formation and hyphal growth. Extracellular phospholipase (*PLP1*) contributes to virulence by degrading host membranes and facilitating tissue invasion (Schena *et al.,* 2023). Metallo-antifungal treatments may modulate the expression of these genes, reducing adhesion, biofilm formation, and tissue invasion (Monteiro *et al.*, 2009). A PCR-based molecular technique enables precise gene expressions to understand better the metal ions' impact on fungal growth and virulence mechanisms (Carvalho *et al.*, 2007; and Makled *et al.*, 2024).

The present work aims to evaluate the antifungal potential of various metal treatments, singly or in combination, against *C. albicans* and *C. tropicalis*. The study also investigated the impact of these treatments on fungal growth, biofilm formation, and the expression of key virulence genes.

MATERIALS AND METHODS

Clinical Sampling

The samples were collected from the Clinical Pathology Lab, Qasr Al-Aini Hospital, Faculty of Medicine, Cairo University. The cultures were cultured and maintained on Sabouraud dextrose agar (SDA) and incubated at 30ºC for 24 to 48 hours.

Antimicrobial Susceptibility Testing (AST)

The Mueller-Hinton agar plates were subjected to 16 antimicrobial compounds to select the most resistant strains. Those antimicrobial compounds were antimicrobial susceptibility testing which was done on the Mueller–Hinton agar plates by disk diffusion (DD) agar method against 16 following antimicrobials: levofloxacin (LEV; 5 µg); ceftazidime (CAZ; 30 µg), cefotaxime (CTX; 30 µg), cefepime (FEP; 30 µg), ertapenem (ETP; 10 µg), amikacin (AK; 30 µg), meropenem (MER; 10 µg), ceftriaxone (CRO; 30 µg), ampicillin/sulbactam (SAM; 10/10 µg), cefoperazone (CFP; 75 µg), imipenem (IPM; 10 µg), nitrofurantoin (NIT; 300 µg), gentamicin (GM; 10 µg), ciprofloxacin (CIP; 5 µg), tetracycline (TET; 30 µg), and trimethoprim-sulfamethoxazole (SXT; 1.25/23.75 µg) according to Basak *et al.* (2016).

Phenotypic Identification

Colony Morphology on SDA and CHROMagar

Every sample was inoculated into Sabouraud dextrose broth (SDB) tubes for 24 hrs. at 30°C, and then the tubes were visually inspected for turbidity. The turbidity-positive cultures were detected. A loopful from each turbid SDB tube was streaked on SDA medium (lot number 1594522/Oxoid) containing chloramphenicol (16 mg/mL, Neo Quimica) according to the method of Marinho *et al.* (2010). The plates were then incubated for 48 hrs. at 30°C. Each grown colony was examined for size, color, and form. *C. albicans* colonies appeared creamy, smooth, and pasty, with a size of approximately 1–3 mm in diameter, whereas *C. tropicalis* colonies were cream to beige, soft, and slightly mucoid, measuring 1-2 mm in diameter. Each SDA plate produced a single colony, which was picked and streaked on the CHROMagar plate (CONDA, Spain), and then the plates were incubated for 48 hrs. at 37°C. On CHROMagar *Candida*, *C. albicans* colonies appeared green, while *C. tropicalis* colonies exhibited dark blue to metallic blue pigmentation.

Microscopic Identifications

Gram Staining: One colony from each SDA plate was streaked on a sterile glass slide, stained using the Gram staining technique, and seen under an oil immersion lens for microscopic examination.

Test in a Germ Tube: One colony was picked from each SDA plate and cultured for two to three hours at 37°C in an Eppendorf tube with 0.5 mL of human serum. Following incubation, a loopful from each Eppendorf tube was inspected under a microscope (Souza, 1998).

Chlamydospores-Forming Test: The test was performed using rice extract agar medium (REA) (10 g rice, 10 g bacteriological agar, and distilled water adjusted to a final volume of 1000 mL) supplemented with 8 mL of Tween 80 (Montes *et al.*, 2019). One single colony from the SDA plate was streaked (very thinly) on the surface of the REA plate in 3-4 broad zigzag lines, then covered with cover glass, and incubated for 9 hrs. at 22–25°C, and then the plate was examined microscopically.

Biotyping

The biotyping process used API 20C Aux strips (bioMérieux, France) to identify the presence or absence of hyphal/pseudohyphal formation. A single colony from a young *Candida* isolated culture was picked from the SDA plate and submerged in an API 20C suspension tube. After filling the strip's cupules with an API 20C medium tube suspension, the API strips were incubated for 24, 48, and 72 hours at 30°C. Following incubation, cupules' turbidity was noted.

Heavy Metals Impacts

Chemical compounds $Na_2B_4O_5$, K_2CrO_4, $FeCl_3$, $C_{12}H_{12}Fe_2O_{18}$, $CoCl_2{\cdot}6H_2O$, $NiCl_2{\cdot}6H_2O$, $CuCl_2{\cdot}2H_2O$, $CuSO_4{\cdot}2H_2O$, $Zn(CH_3COO)_2$, $(NH_4)_6Mo_7O_{24}.4H_2O$, and Na_2MoO_4 were used at concentrations of 0.1 M either singly or in combination on the selected resistant species. The valency of an element in a compound can vary based on its location in the periodic table and other constituents' charges, with elements like iron and manganese exhibiting multiple oxidation states. $Na_2B_4O_5$, K_2CrO_4, $FeCl_3$, $C_{12}H_{12}Fe_2O_{18}$, $CoCl_2{\cdot}6H_2O$, $NiCl_2{\cdot}6H_2O$, $CuCl_2{\cdot}2H_2O$, $CuSO_4{\cdot}2H_2O$, $Zn(CH_3COO)_2$, $(NH_4)_6Mo_7O_{24}.4H_2O$, and Na_2MoO_4 metals were assigned as B, Cr, Fe1, Fe2, Co, Ni, Cu1, Cu2, Zn, Mo1, and Mo2, respectively.

Disc Diffusion Method

Disc diffusion (DD) agar was used to confirm and measure the best treatment's antifungal activity. The microdilution technique was used to estimate the minimum inhibitory and fungicidal concentrations (MIC and MFC) according to Marinho *et al.* (2010) and Wang *et al.* (2025). Sterile filter paper discs (6 mm diameter) were impregnated with 20 µL of 0.1 M solutions of the best treatment. The discs were air-dried under sterile conditions before being placed on Sabouraud dextrose agar (SDA) plates preinoculated with *Candida albicans* or *Candida tropicalis* suspensions (0.5 McFarland standard). The plates were incubated at 30°C for 24–48 hours, after which the inhibition zones (IzD) were measured in millimeters using a ruler.

Molecular Analysis cPCR

The whole genomic DNA of *C. albicans* and *C. tropicalis* was extracted following the guidelines provided by QIAamp DNA Mini Kit catalogue no. 51304.

***Candida* Species Identification and Virulence Genes Detection**

The Emerald Amp GT PCR master-mix (Takara) code no. RR310A kit was used to prepare the PCR master mix. Oligonucleotide primers used in cPCR are specially constructed with distinct sequences to amplify certain products (Table 1). In an iced PCR tube, the reaction mixture comprised 12.5 µL PCR master mix (2x), 2 µL forward and reverse primer (20 pmol), 5 µL template DNA, and 5.5 µL PCR-grade water, forming a 25 µL total volume. The cPCR amplification was performed using a thermal cycler, as presented in Table 2. PCR products were separated by electrophoresis (3 hrs., 80 v) through 1.5% agarose in 1x TAE buffer (40 mM Tris base, 20 mM acetic acid, and 1 mM EDTA, pH 8.0) according to Sambrook *et al.*'s (1989) methodology. Band sizes were visualized and determined based on a 100 bp DNA ladder (cat. no. SM0243) from Fermentas.

Real-Time PCR

Total RNA was extracted from *C. albicans* and *C. tropicalis* using the guidelines for the RNeasy Mini Kit (Qiagen, cat. no. 74104) and lysozyme (AppliChem, cat. no. A3711). After purity and concentration check using a Nanodrop spectrophotometer (ND-2000 c, Thermo Fisher Scientific, Wilmington, DE, USA), one µg RNA of each sample was reverse-transcribed into cDNA employing RevertAid Reverse Transcriptase (Thermo Fisher, cat. no. EP0441). Preparation of PCR master mix was done according to Quantitect SYBR Green PCR kit. The reaction mixture comprised 12.5 µL 2x QuantiTect SYBR Green PCR master mix (cat. no. 204141), 0.25 µL reverse transcriptase, 1 µL forward and reverse primers (20 pmol), 3 µL template RNA, and 8.25 µL RNase-free water (Qiagen, cat. no. 79254) forming a 25 µL total volume. Quantitative amplifications were implemented using a Stratagene MX3005P real-time system (CA, USA) employing specific primers listed in Table 3. After examining the SYBR Green rt-PCR findings, the Stratagene MX3005P program was used to determine the Ct values and amplification curves. Using the "ΔΔ Ct" method described by Yuan *et al.* (2006), the Ct of each sample was compared with that of the control group to estimate the variation of gene expression on the RNA of the various samples.

whereas ΔΔ Ct = Δ Ct reference – Δ Ct target,
Δ Ct target = Ct control – Ct treatment, and
Δ Ct reference = Ct control – Ct treatment.
To rule out false positive results, dissociation curves were compared across samples.

Statistical Analysis

Sigma Plot (Systat Software) was used for statistical analysis. Where applicable, statistical significance was determined by Tukey's honestly significant difference

Table 1. Oligonucleotide primers sequences (Metabion, Germany).

Microbe	Gene	Sequence	Amplified product (bp)	Reference
C. albicans *C. tropicalis*	*SAP4*	GCT CTT GCT ATT GCT TTA TTA	394	Sikora *et al*. (2011)
		TAG GAA CCG TTA TTC TTA CA		
	ALS1	GAC TAG TGA ACC AAC AAA TAC CAG A	318	İnci *et al.* (2013)
		CCA GAA GAA ACA GCA GGT GA		
	HWP1	ATG ACT CCA GCT GGT TC	572	
		TAG ATC AAG AAT GCA GC		
	ALS3	CTGGACCACCAGGAAACACT	122	Tsang *et al.* (2012)
		ACCTGGAGGAGCAGTGAAAG		
	RAS1	CCCAACTATTGAGGATTCTTATCGTAAA	106	
		TCTCATGGCCAGATATTCTTCTTG		
	Hyr1	CGTCAACCTGACTGTTACATC	243	Luo *et al.* (2010)
		TCTACGGTGGTATGTGGAAC		
	Plb1	ATGATTTTGCATCATTTG	751	Mukherjee *et al*. (2001)
		AGTATCTGGAGCTCTACC		
		TTTCGTGTGGCCAGTGACTC		

Table 2. Cycling conditions of the different primers during cPCR.

Microbe	Gene	Primary denaturation	Secondary denaturation	Annealing	Extension	No. of cycles	Final extension
C. albicans *C. tropicalis*	*SAP4*	94℃ 5 min.	94℃ 30 sec.	49℃ 40 sec.	72℃ 40 sec.	35	72℃ 10 min.
	ALS1	94℃ 5 min.	94℃ 40 sec.	50℃ 40 sec.	72℃ 40 sec.	35	72℃ 10 min.
	HWP1	94℃ 5 min.	94℃ 40 sec.	45℃ 40 sec.	72℃ 45 sec.	35	72℃ 10 min.
	ALS3	94℃5 min.	94℃ 30 sec.	60℃ 30 sec.	72℃ 30 sec.	35	72℃ 7 min.
	RAS1	94℃ 5 min.	94℃ 30 sec.	60℃ 30 sec.	72℃ 30 sec.	35	72℃ 7 min.
	Hyr1	94℃ 5 min.	94℃ 30 sec.	55℃ 30 sec.	72℃ 30 sec.	35	72℃ 7 min.
	Plb1	94℃ 5 min.	94℃ 40 sec.	50℃ 40 sec.	72℃ 45 sec.	35	72℃ 10 min.

Table 3. Oligonucleotide primers and probes used in SYBR Green real-time PCR.

Gene	Primer sequence (5'-3')	Reference
SAP4	GCT CTT GCT ATT GCT TTA TTA	Sikora *et al.* (2011)
	TAG GAA CCG TTA TTC TTA CA	
ALS1	GAC TAG TGA ACC AAC AAA TAC CAG A	İnci *et al.* (2013)
	CCA GAA GAA ACA GCA GGT GA	
HWP1	ATG ACT CCA GCT GGT TC	
	TAG ATC AAG AAT GCA GC	
HYR1	CGTCAACCTGACTGTTACATC	Luo *et al.* (2010)
	TCTACGGTGGTATGTGGAAC	
PLB1	ATGATTTTGCATCATTTG	Mukherjee *et al.* (2001)
	AGTATCTGGAGCTCTACC	
ITS	GGTTTGCTTGAAAGACGGTAG	Tarini *et al.* (2010)
	AGTTTGAAGATATACGTGGTAG	

The amplification protocol is listed in Table 4.

Table 4. Cycling conditions for SYBR Green real-time PCR

Target gene	Reverse transcription	Primary denaturation	Amplification (40 cycles)			Dissociation curve (1 cycle)		
			Secondary denaturation	Annealing (optics on)	Extension	Secondary denaturation	Annealing	Final denaturation
SAP4	50℃ 30 min.	94℃ 15 min.	94℃ 15 sec.	49℃ 30 sec.	72℃ 40 sec.	94℃ 1 min.	49℃ 1 min.	94℃ 1 min.
ALS1				50℃ 30 sec.			50℃ 1 min.	
HWP1				45℃ 30 sec.			45℃ 1 min.	
HYR1				55℃ 30 sec.			55℃ 1 min.	
PLB1				50℃ 30 sec.			50℃ 1 min.	
ITS				50℃ 30 sec.			50℃ 1 min.	

(HSD) test following an F test. *P* values of less than 0.05 are considered important. All data presented are mean values, with error bars representing standard errors of the means (SEM) from at least three biological replicates.

RESULTS

Antimicrobial susceptibility testing performed using the disk diffusion (DD) agar method at the Clinical Pathology Lab, Qasr Al-Aini Hospital, Faculty of Medicine, Cairo University, showed that *C. albicans* and *C. tropicalis* were the most resistant strains isolated from the collected samples. Figure 1 represents the PCR-based identification of *C. albicans* and *C. tropicalis*. DNA band intensities corresponding to species-specific amplification products were observed, verifying the identity of these isolates: 109 bp band for *C. albicans* and 130 bp band for *C. tropicalis*. The PCR products appeared at 110 bp for *C. tropicalis* and 109 bp for *C. albicans*, confirming their identification. The antifungal activity of single and combined metal ions against *C. albicans* was illustrated in Figure 2 as inhibition zone diameters (IzD). Among the tested single metals, chromium (Cr) exhibited the most considerable IzD value (19 mm), followed by cobalt (Co; 10 mm), boron (B; 9 mm), nickel (Ni; 8 mm), and molybdenum (Mo2; 8 mm) with moderate inhibition zones. Copper (Cu1, Cu2) and molybdenum (Mo1) exhibited a lower effect (6 mm). However, iron (Fe1 and Fe2) and zinc (Zn) had no inhibitory effect.

Among the Co combinations, Mo1 exhibited the most potent inhibitory effect (24 mm), which appeared synergistic compared to their high individual effects (10 mm for Co versus 6 mm for Mo1). The Co/Cr combination showed slightly higher inhibition than Ni alone (20 mm versus 19 mm), indicating a mild synergistic effect. The same also occurred in Co/B combination (11 mm versus 9 mm). When Co was combined with copper (Cu1) or zinc (Zn), the inhibition zone increased moderately compared to copper or zinc alone (7 mm versus 6 mm or 6 mm versus 0 mm, respectively). Co/Fe1 combination was a great sign for no inhibitory effect to moderate inhibition zone (9 mm versus 0 mm), while Co/Cu2 and Co/Mo2 exhibited an antagonistic effect compared to single effect (0 mm versus 6 mm, and 6 mm versus 8 mm, respectively). Concerning the combination with Mo1, Co exhibited the most potent inhibitory effect (24 mm); on the other hand, an antagonistic effect was shown in the inhibition zone when Mo1 was combined with other single metals.

Figure 3 demonstrates the inhibition zone diameters (IzD) of *C. tropicalis* influenced by single and combined metal treatments. Among the tested metals, chromium (Cr) exhibited the most considerable IzD value (19 mm), followed by cobalt (Co) exhibiting an IzD value of 10 mm, boron (B) exhibiting an IzD value of 9 mm, and then nickel (Ni) and molybdenum (Mo2) with moderate inhibition zones (8 mm). Copper (Cu2) and molybdenum (Mo1) exhibited a lower effect (6 mm). However, iron (Fe2) and zinc (Zn) had no inhibitory effect. Combining Mo1 with Co significantly increased inhibition (about 23 mm), suggesting a synergistic antifungal effect. The Co/Cr combination exhibited a slight increase in the inhibition zone compared to the single Cr treatment, followed by Co/Ni and Co/B combination which was moderately synergetic. Fe1 maintained moderate activity while Fe2 remained ineffective even when combined with Co. Copper (Cu1 and Cu2) and zinc (Zn) had relatively low inhibition zones, an antagonistic effect regardless of whether they were combined with Co or Mo1. Zinc (Zn) had no antifungal activity either singly or in combination, but in combination with Co it showed slight synergism. Mo1/Mo2 combination displayed minimal inhibition compared to Mo1 alone.

Finally, Mo1 and Co exhibited vigorous antifungal activity on both *Candida* species, especially in combination (Figures 2 and 3). Due to their antifungal efficacy, this combination was used for further investigation. Disc diffusion (DD) agar was used to confirm and measure the antifungal activity of the Co/Mo combination against *C. albicans* and *C. tropicalis* (Figure 4) as minimum inhibitory and fungicidal concentrations (MIC and MFC). The results confirmed the potent antifungal properties of the Co/Mo combination at 58.93 µg/mL (0.001 M Co) and 95.95 µg/mL (0.001 M Mo), with no fungicidal effect below 0.1 M. Figure 5 illustrates the PCR results for virulence genes (*RAS1*, *HWP1*, *ALS3*, *SAP4*, and *HYR1*), and Table 5 summarizes the gene presence (+) or absence (-) in *C. albicans*. The amplification of the adhesion- and the virulence-related genes in *C. albicans* indicated the amplification of *HWP1*, *HYR1*, and *SAP4* genes and the absence of *RAS1* and *ALS3* genes.

Table 6 presents the fold changes in gene expression of *C. albicans*, and Figure 6 shows the genes' amplification curves with *ITS* used as a reference. Under metal treatment, *HWP1* gene expression was downregulated by about 50%, *SAP4* gene expression decreased by about 80%, and *HYR1* gene expression

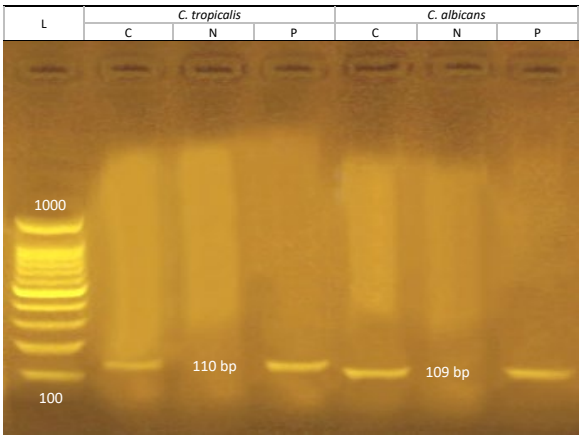

Figure 1. PCR-based identification of *Candida tropicalis* and *Candida albicans*

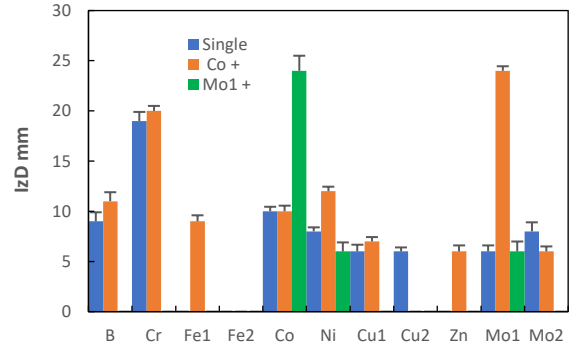

Figure 2. Impact of various single metals on the inhibition zone diameter (IzD, mm) of *Candida albicans*

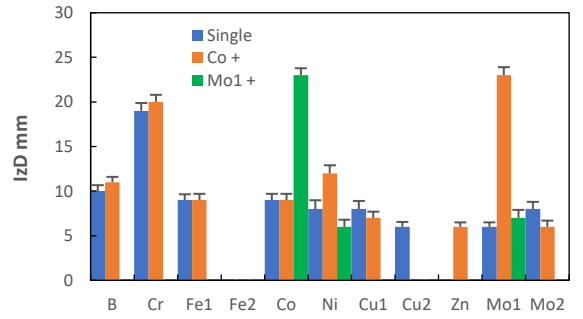

Figure 3. Impact of various single metals on the inhibition zone diameter (IzD, mm) of *C. tropicalis*

Figure 4. Antimicrobial activity of Co/Mo combination against *C. albicans* and *C. tropicalis*

Table 5. PCR analysis results for various genes in *C. albicans.*

C. albicans	*Hyr*1	*RAS1*	*ALS3*	*HWP1*	*SAP4*
C	+	-	-	+	+

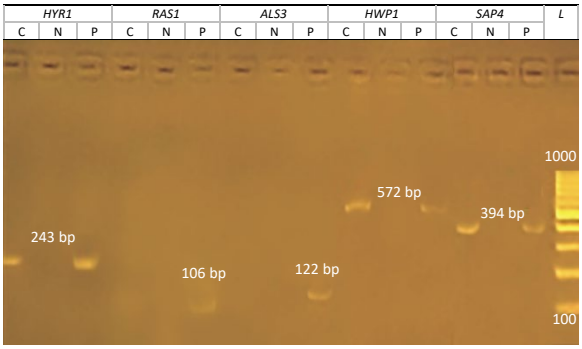

Figure 5. PCR analysis for various genes in *C. albicans*

was downregulated. Table 7 and Figure 7 demonstrate the PCR analysis used to identify the genes associated with pathogenicity and biofilm formation in *C. tropicalis*. The PCR results confirmed the presence of *ALS1* and *PLB1* genes and the absence of *RAS1* and *ALS3* genes. Table 8 outlines the fold changes in gene expression of *C. tropicalis*, and Figure 8 shows the genes' amplification curves with *ITS* used as a reference. *ALS1* expressions are downregulated by about 90% under metal treatment, and *PLB1* expression shows an 80% reduction.

Table 6. Quantitative PCR (qPCR) shows genes' expression levels in *C. albicans*

C. albicans	*ITS*	*SAP4*		*HWP1*		*HYR1*	
	CT	CT	Fold change	CT	Fold change	CT	Fold change
CC	19.83	22.35	-	20.77	-	21.80	-
CT	19.57	24.35	0.2088	21.43	0.5285	22.72	0.4414

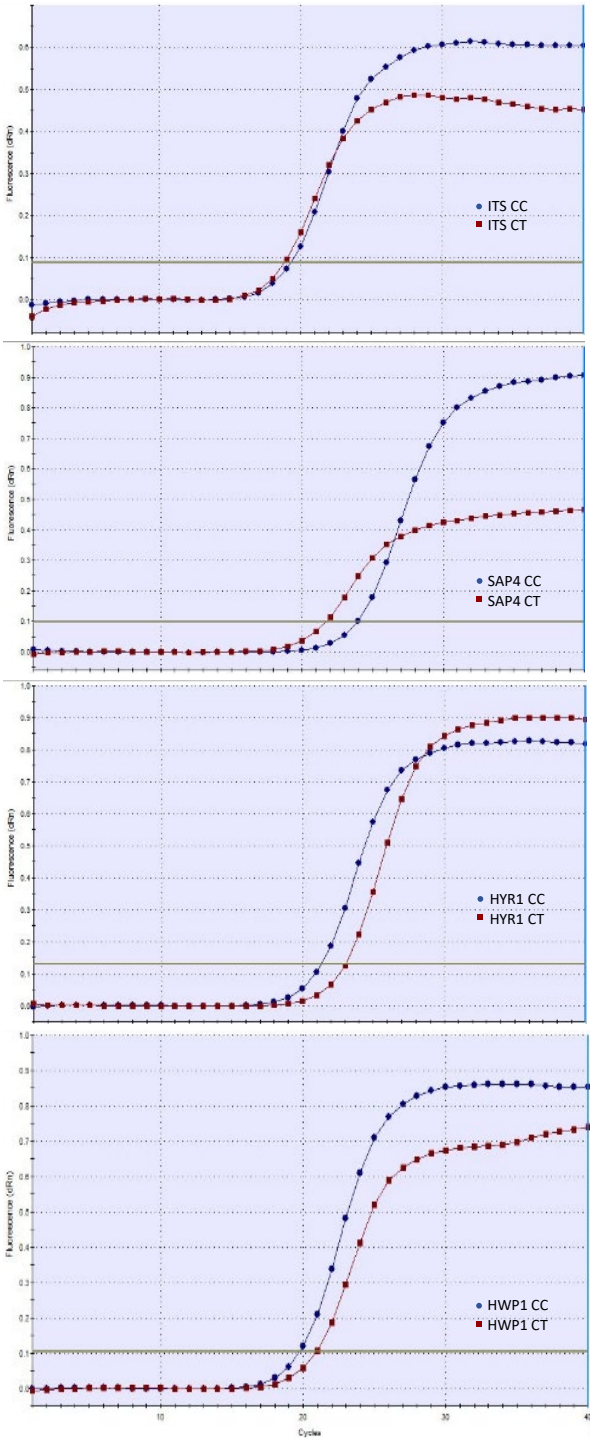

Figure 6. Amplification plots show the expression of the *ITS, SAP4, HYR1, and HWP1* genes in *C. albicans.*

Table 7. PCR analysis results for various genes in *C. tropicalis.*

C. tropicalis	*Plb1*	*RAS1*	*ALS3*	*ALS1*
C	+	-	-	+

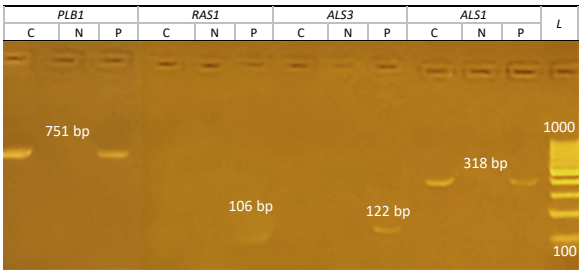

Figure 7. PCR analysis of various genes in *C. tropicalis.*

Table 8. Quantitative PCR (qPCR) shows the expression levels of several genes in *C. tropicalis*

C. tropicalis	*ITS*	*ALS1*		*PLB1*	
	CT	CT	Fold change	CT	Fold change
CC	19.83	21.42	-	23.91	-
CT	19.57	24.20	0.1216	25.85	0.2176

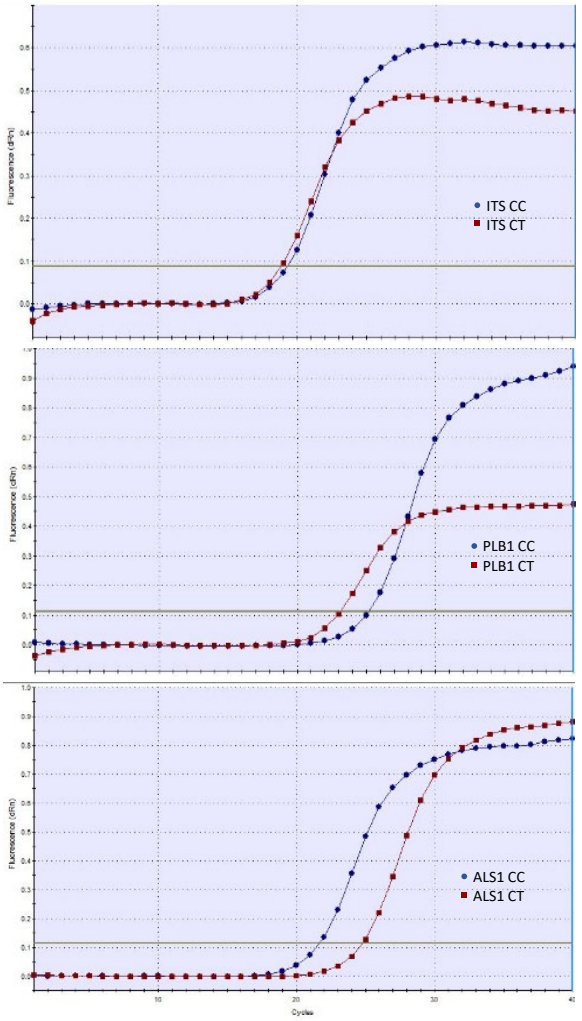

Figure 8. Amplification plots show the expression of the *ITS*, *PLB1*, *and ALS1* genes in *C. tropicalis*

DISCUSSION

Metal Sensitivity and Resistance Patterns

PCR-based identification confirmed the identification of *C. albicans* and *C. tropicalis*, with DNA bands corresponding to species-specific amplification products: 110 bp for *C. tropicalis* and 109 bp for *C. albicans.* Carvalho *et al.* (2007) reported the reliability of PCR-based identification in confirming *Candida* species identity. As assessed by inhibition zone diameters (IzD), the antifungal activity of single metals revealed that chromium showed the most significant antifungal effects. These results suggest that specific metals may disrupt fungal cell viability by disrupting essential processes like metal homeostasis, oxidative stress balance, and enzyme function (Mayer *et al.,* 2013; and Dutta *et al.,* 2018).

Synergistic Effects of Co/Mo Treatment

The antifungal activity of single metal ions, as assessed by inhibition zone diameters (IZD), revealed that chromium, molybdenum, and cobalt showed the most significant antifungal effects. These results suggest that certain metal ions may disrupt fungal cell viability by disrupting essential processes like metal homeostasis, oxidative stress balance, and enzyme function (Robinson *et al.,* 2021). The present study found that combining cobalt or molybdenum enhanced inhibition of *Candida* species (Quaranta *et al.*, 2011) and competition for metal transporters are likely contributing to this. The combination of Zn with either Co or Mo1 exhibited low inhibition zones (Schwartz *et al.*, 2013). This suggests that Zn might interfere with their antifungal activity, possibly due to competition for cellular uptake or binding sites. Metal cations may compete with more active metal ions for transport mechanisms in fungal cells, which could lessen the toxicity of the latter (Campbell *et al.*, 2022). The combination of different molybdenum sources (Mo1 and Mo2) results in the formation of minimal inhibition. The two molybdenum sources have identical mechanisms of action, which creates a redundancy that prevents the combined antifungal effects from being strengthened. This observation aligns with the understanding that antifungal agents targeting the same cellular processes can exhibit overlapping effects, limiting their combined efficacy (Prasad *et al.*, 2016). The combination of Mo1 with Co exhibited the most potent inhibition (24 mm IzD) compared to their single impacts, suggesting a synergistic effect. Enhanced antifungal activity in *Candida* species may be due to disruption of the cell membrane integrity, interference with cellular metal transport mechanisms, induced oxidative stress, or disruption of essential enzymatic pathways for fungal growth and survival (Turecka *et al.*, 2018).

Downregulation of Virulence Genes and Implications

Gene expression demonstrated that the Co/Mo1 combination drastically downregulated critical virulent genes in *Candida* species. The downregulation of *HYR1* (hyphal growth), *SAP4* (protease), and *HWP1* (adhesion) in *C. albicans* suggests a diminished capacity to infiltrate host tissues and produce biofilms. In *C. tropicalis*, *ALS1* (adhesion) and *PLB1* (phospholipase) were also strongly inhibited, further supporting the antifungal potential of metal ions in lowering fungal pathogenicity. Virulence factors such as adhesion, biofilm formation, and enzymatic degradation of host tissues are essential for *Candida* pathogenicity (Sobieh *et al.,* 2024). Suppressing these genes indicates that the Co/Mo combination inhibits fungal growth and impairs its ability to colonize and infect host tissues. *C. albicans* has significantly reduced pathogenic potential due to the downregulation of *HYR1*, *SAP4*, and *HWP1* genes. *HYR1* is crucial for tissue invasion and immune evasion (Granger *et al.*, 2005), while *SAP4* inhibits host protein degradation, reducing the ability of *C. albicans* to evade immune responses (Naglik *et al.,* 2003). *HWP1* is essential for biofilm development and host attachment (Finkel and Mitchell, 2011). These downregulations suggest that metal ions interfere with key virulence traits. The suppression of *ALS1* and *PLB1* in *C. tropicalis* reveals the antifungal properties of metal ions in the Co/Mo1 combination. *ALS1* is crucial for biofilm formation and host colonization while *PLB1* is essential for membrane degradation and penetration into host tissues (Arafa *et al.,* 2023).

Mechanistic Insights on Metal-Fungal Interaction

The Co/Mo combination impairs fungal adhesion, making *C. tropicalis* less susceptible to persistent infections. Metal-induced stress can disrupt the cAMP-PKA signaling pathway, which regulates morphogenesis and virulence in *C. albicans*, leading to downregulation of adhesion, hyphal development, and enzymatic activity. Metals like cobalt and molybdenum generate reactive oxygen species, leading to oxidative damage and altered gene expression (Thomas and Wigneshweraraj, 2014; Dantas *et al.,* 2015; and da Silva *et al.*, 2022). The Hog1 mitogen-activated protein kinase pathway may suppress virulence factors (Komath, 2024).

Absence of *RAS1* and *ALS3* Genes and Its Impact

The results also revealed the absence of *RAS1* and *ALS3* genes in *C. albicans* and *C. tropicalis* under Co/Mo1 combination treatment, which could impact fungal virulence. *RAS1* regulates morphogenesis and the cAMP-PKA signaling pathway, controlling the yeast-to-hypha transition (Grahl *et al.,* 2015). The expression of several cell surface proteins, notably the hypha-specific protein *AlS3*p, is necessary to produce biofilms in this organism. Cell-cell adhesion is reduced, and biofilm formation is hampered by *ALS3* loss. The absence of both *RAS1* and *ALS3* could potentially reduce the pathogenicity of *Candida* species and decrease its adhesion and invasion capabilities, which could contribute to the downregulation of virulence factors upon metal treatment (Schena *et al.,* 2023).

CONCLUSION

The study reveals the potent antifungal activity of specific metal ions, particularly the Co/Mo combination, followed by Co/Cr, against *Candida albicans* and *Candida tropicalis*. Single treatments of chromium, nickel, and cobalt showed significant inhibitory effects, while zinc and ferrous showed no antifungal activity individually. The synergistic action of Co and Mo1 resulted in the most potent inhibition, highlighting their potential as antifungal agents. Gene expression analysis revealed that Co/Mo treatment significantly downregulated key virulent genes in *Candida* species, reducing their ability to form biofilms and invade host tissues. Finally, Co/Mo-based treatment could be a promising alternative antifungal strategy, particularly for drug-resistant *Candida* infections.

REFERENCES

Arafa, S.H., Elbanna, K., Osman, G.E.H., Abulreesh, H.H. (2023) *Candida* diagnostic techniques: a review. *Journal of Umm Al-Qura University for Applied Sciences*; (9), 360–377.

Basak, S., Singh, P., Rajurkar, M. (2016) Multidrug Resistant and Extensively Drug-Resistant Bacteria: A Study. *Journal of pathogens*, *2016*, 4065603.

Butler, G., Rasmussen, M. D., Lin, M. F., Santos, M. A., Sakthikumar, S., Munro, C. A., Rheinbay, E., Grabherr, M., Forche, A., Reedy, J. L., Agrafioti, I., Arnaud, M. B., Bates, S., Brown, A. J., Brunke, S., Costanzo, M. C., Fitzpatrick, D. A., de Groot, P. W., Harris, D., Hoyer, L. L., Cuomo, C. A. (2009) Evolution of pathogenicity and sexual reproduction in eight *Candida* genomes. *Nature*, *459*(7247), 657–662.

Campbell, J. X., Gao, S., Anand, K. S., Franz, K. J. (2022) Zinc Binding Inhibits Cellular Uptake and Antifungal Activity of Histatin-5 in *Candida albicans*. *ACS infectious diseases*, *8*(9), 1920–1934.

Carvalho, A., Costa-De-Oliveira, S., Martins, M. L., Pina-Vaz, C., Rodrigues, A. G., Ludovico, P., Rodrigues, F. (2007) Multiplex PCR identification of eight clinically relevant Candida species. *Medical mycology*, *45*(7), 619–627. https://doi.org/10.1080/13693780701501787

Černáková, L., Rodrigues, C. F. (2020) Microbial interactions and immunity response in oral *Candida* species. *Future microbiology*, *15(/7)*, 1653–1677

Chandra, J., Kuhn, D. M., Mukherjee, P. K., Hoyer, L. L., McCormick, T., Ghannoum, M. A. (2001) Biofilm formation by the fungal pathogen *Candida albicans*: development, architecture, and drug resistance. *Journal of bacteriology*, *183*(18), 5385–5394.

Colombo, A. L., Guimarães, T., Silva, L. R., de Almeida Monfardini, L. P., Cunha, A. K., Rady, P., Alves, T., Rosas, R. C. (2007) Prospective observational study of candidemia in São Paulo, Brazil: incidence rate, epidemiology, and predictors of mortality. *Infection control and hospital epidemiology*, *28*(5), 570–576.

Dantas, A.daS., Day, A., Ikeh, M., Kos, I., Achan, B., Quinn, J. (2015) Oxidative stress responses in the human fungal pathogen, *Candida albicans*. *Biomolecules*, *5*(1), 142–165.

da Silva, D. C. B., Garnelo, L., Herkrath, F. J. (2022) Barriers to Access the Pap Smear Test for Cervical Cancer Screening in Rural Riverside Populations Covered by a Fluvial Primary Healthcare Team in the Amazon. *International journal of environmental research and public health*, *19*(7), 4193.

Dutta, S., Mitra, M., Agarwal, P., Mahapatra, K., De, S., Sett, U., Roy, S. (2018) Oxidative and genotoxic damages in plants in response to heavy metal stress and maintenance of genome stability. *Plant signaling & behavior*, *13*(8), e1460048.

Finkel, J. S., Mitchell, A.P. (2011) Genetic control of *Candida albicans* biofilm development. *Nature reviews. Microbiology*, *9*(2), 109–118.

Gácser, A., Schäfer, W., Nosanchuk, J. S., Salomon, S., Nosanchuk, J. D. (2007a) Virulence of *Candida parapsilosis, Candida orthopsilosis,* and *Candida metapsilosis* in reconstituted human tissue models. *Fungal genetics and biology : FG & B*, *44*(12), 1336–1341.

Gácser, A., Trofa, D., Schäfer, W., & Nosanchuk, J. D. (2007b) Targeted gene deletion in *Candida parapsilosis* demonstrates the role of secreted lipase in virulence. *The Journal of clinical investigation*, *117*(10), 3049–3058.

Grahl, N., Demers, E. G., Lindsay, A. K., Harty, C. E., Willger, S. D., Piispanen, A. E., Hogan, D. A. (2015) Mitochondrial Activity and *Cyr*1 Are Key Regulators of *Ras*1 Activation of *C. albicans* Virulence Pathways. *PLoS pathogens*, *11*(8), e1005133.

Granger, B. L., Flenniken, M. L., Davis, D. A., Mitchell, A. P., Cutler, J. E. (2005) Yeast wall protein 1 of *Candida albicans*. *Microbiology*, *151*(5), 1631-1644.

İnci, M.; Atalay, M. A.; Özer, B.; Evirgen, Ö.; Duran, N.; Motor, V. K.; Koç, A. N.; Önlen, Y.; Kilinç, Ç.; and Durmaz, S. (2013) "Investigations of *ALS*1 and *HWP*1 genes in clinical isolates of *Candida albicans*," *Turkish Journal of Medical Sciences*: Vol. 43: No. 1, Article 22.

Klesiewicz, K., Mrowiec, P., Kania, K., Skiba-Kurek, I., Białecka, J., Namysł, M., Małek, M. (2023) Prevalence of Closely Related *Candida albicans* Species among Patients with Vulvovaginal Candidiasis in Southern Poland Based on the *hwp*1 Gene Amplification. *Polish journal of microbiology*, *72*(1), 69–77.

Komath S. S. (2024) To each its own: Mechanisms of crosstalk between GPI biosynthesis and cAMP-PKA signaling in *Candida albicans* versus *Saccharomyces cerevisiae*. *The Journal of biological chemistry*, *300*(7), 107444.

Luo, G., Ibrahim, A. S., Spellberg, B., Nobile, C. J., Mitchell, A. P., Fu, Y. (2010) *Candida albicans Hyr*1p confers resistance to neutrophil killing and is a potential vaccine target. *The Journal of infectious diseases*, *201*(11), 1718–1728.

Makled, A.F., Ali, S.A.M., Labeeb, A.Z., Salman, S.S., Shebl, D.Z.M.,Hegazy, S.G. Sabal, M.S. (2024) Characterization of *Candida* species isolated from clinical specimens: insights into virulence traits, antifungal resistance and molecular profiles. *BMC Microbiology,* 24, 388 (2024).

Marinho, S. A., Teixeira, A. B., Santos, O. S., Cazanova, R. F., Ferreira, C. A., Cherubini, K., de Oliveira, S. D. (2010) Identification of *Candida* spp. by phenotypic tests and PCR. *Brazilian journal of microbiology: [publication of the Brazilian Society for Microbiology]*, *41*(2), 286–294.

Mayer, F. L., Wilson, D., & Hube, B. (2013) *Candida albicans* pathogenicity mechanisms. *Virulence*, *4*(2), 119–128.

Monteiro, D. R., Gorup, L. F., Takamiya, A. S., Ruvollo-Filho, A. C., de Camargo, E. R., Barbosa, D. B. (2009) The growing importance of materials that prevent microbial adhesion: antimicrobial effect of medical devices containing silver. *International journal of antimicrobial agents*, *34*(2), 103–110.

Montes, K., Ortiz, B., Galindo, C., Figueroa, I., Braham, S., Fontecha, G. (2019). Identification of *Candida* Species from Clinical Samples in a Honduran Tertiary Hospital. *Pathogens (Basel, Switzerland)*, *8*(4), 237.

Mukherjee, P. K., Seshan, K. R., Leidich, S. D., Chandra, J., Cole, G. T., Ghannoum, M. A. (2001) Reintroduction of the *PLB1* gene into *Candida albicans* restores virulence in vivo. *Microbiology (Reading, England)*, *147*(Pt 9), 2585–2597.

Naglik, J. R., Challacombe, S. J., Hube, B. (2003) *Candida albicans* secreted aspartyl proteinases in virulence and pathogenesis. *Microbiology and molecular biology reviews : MMBR*, *67*(3), 400–428.

Orsi, C. F., Borghi, E., Colombari, B., Neglia, R. G., Quaglino, D., Ardizzoni, A., Morace, G., Blasi, E. (2014) Impact of *Candida albicans* hyphal wall protein 1 (*HWP1*) genotype on biofilm production and fungal susceptibility to microglial cells. *Microbial pathogenesis*, *69-70*, 20–27.

Pappas, P. G., Kauffman, C. A., Andes, D. R., Clancy, C. J., Marr, K. A., Ostrosky-Zeichner, L., Reboli, A. C., Schuster, M. G., Vazquez, J. A., Walsh, T. J., Zaoutis, T. E., Sobel, J. D. (2016) Clinical Practice Guideline for the Management of Candidiasis: 2016 Update by the Infectious Diseases Society of America. *Clinical infectious diseases: an official publication of the Infectious Diseases Society of America*, *62*(4), e1–e50.

Prasad, R., Shah, A. H., Rawal, M. K. (2016) Antifungals: Mechanism of Action and Drug Resistance. *Advances in experimental medicine and biology*, *892*, 327–349.

Quaranta, D., Krans, T., Espírito Santo, C., Elowsky, C. G., Domaille, D. W., Chang, C. J., Grass, G. (2011) Mechanisms of contact-mediated killing of yeast cells on dry metallic copper surfaces. *Applied and environmental microbiology*, *77*(2), 416–426.

Robinson, J. R., Isikhuemhen, O. S., Anike, F. N. (2021) Fungal–Metal Interactions: A Review of Toxicity and Homeostasis. *Journal of Fungi*, *7*(3), 225.

Sambrook J., Fritscgh E.F., and Mentiates (1989) Molecular coloning. A laboratory manual. Vol! *Cold Spring Harbor Laboratory Press*, New York.

Schena NC, Baker KM, Stark AA, Thomas DP, Cleary IA (2023) Constitutive *ALS3* expression in *Candida albicans* enhances adhesion and biofilm formation of *efg1*, but not *cph1* mutant strains. *PLoS ONE*, 18(7): e0286547.

Schwartz, J. A., Olarte, K. T., Michalek, J. L., Jandu, G. S., Michel, S. L., Bruno, V. M. (2013) Regulation of copper toxicity by *Candida albicans GPA*2. *Eukaryotic cell*, *12*(7), 954–961.

Sikora, M., Dabkowska, M., Swoboda-Kopec, E., Jarzynka, S., Netsvyetayeva, I., Jaworska-Zaremba, M., Pertkiewicz, M., Mlynarczyk, G. (2011) Differences in proteolytic activity and gene profiles of fungal strains isolated from the total parenteral nutrition patients. *Folia microbiologica*, *56*(2), 143–148.

Silva, S., Negri, M., Henriques, M., Oliveira, R., Williams, D. W., Azeredo, J. (2012) *Candida glabrata, Candida parapsilosis* and *Candida tropicalis*: biology, epidemiology, pathogenicity and antifungal resistance. *FEMS microbiology reviews*, *36*(2), 288–305.

Sobieh, S.S., Elshazly, R.G., Tawab, S.A. & Zakii, S.S. (2024) Estimating the expression levels of genes controlling biofilm formation and evaluating the effects of different conditions on biofilm formation and secreted aspartic proteinase activity in *Candida albicans* and *Saccharomyces cerevisiae*: a comparative study. *Beni-Suef University Journal of Basic and Applied Sciences,* 13, 49.

Souza V.M. (1998) Técnicas laboratoriais utilizadas em micologia médica. In: Zaitz C, Campbell I, Marques AS, Ruiz LR, Souza VM (eds) Compêndio de micologia médica. *Medsi, Rio de Janeiro*, 51–63.

Tarini NMA, Wahid MH, Ibrahim F, Yasmon A, Djauzi S. (2010) Development of multiplex-PCR assay for rapid detection of *Candida* spp. *Medical Journal of Indonesia*, 19(2), 83-7.

Thomas, M. S., Wigneshweraraj, S. (2014) Regulation of virulence gene expression. *Virulence*, *5*(8), 832–834.

Tsang, P. W., Bandara, H. M., & Fong, W. P. (2012). Purpurin suppresses *Candida albicans* biofilm formation and hyphal development. *PloS one*, *7*(11), e50866. https://doi.org/10.1371/journal.pone.0050866

Turecka, K., Chylewska, A., Kawiak, A., Waleron, K. F. (2018) Antifungal Activity and Mechanism of Action of the Co(III) Coordination Complexes with Diamine Chelate Ligands Against Reference and Clinical Strains of *Candida* spp. *Frontiers in microbiology*, *9*, 1594.

Wang, Y., Chen, X., Peng, K., Tie, Y., Gao, Y., Han, Z., Lyu, X., Li, H., Zhang, R., Gao, S., Shen, X., Ma, X., Feng, Z. (2025) Rapid and sensitive identification of *Candida* in blood based on M1 beads enrichment combined with multiple recombinase-aided PCR: a culture-independent approach. *Frontiers in cellular and infection microbiology*, *15*, 1552529.

Yuan, J. S., Reed, A., Chen, F., Stewart, C. N., Jr (2006) Statistical analysis of real-time PCR data. *BMC bioinformatics*, *7*, 85.